Anti-Vascular Endothelial Growth Factor Receptor 2 Antibody Reduces Tumorigenicity and Metastasis in Orthotopic Prostate Cancer Xenografts via Induction of Endothelial Cell Apoptosis and Reduction of Endothelial Cell Matrix Metalloproteinase Type 9 Production[1]

Paul Sweeney, Takashi Karashima, Sun-Jin Kim, Daniel Kedar, Badar Mian, Samuel Huang, Cheryl Baker, Zhen Fan, Daniel J. Hicklin, Curtis A. Pettaway, and Colin P. N. Dinney[2]

Departments of Urology [C. P. N. D.], Cancer Biology [P. S., T. K., S-J. K., D. K., B. M., S. H., C. B., C. A. P.] and Experimental Therapeutics [Z. F.], The University of Texas M. D. Anderson Cancer Center, Houston, Texas 77030, and ImClone Systems, New York, New York 10014 [D. J. H.]

ABSTRACT

Purpose: **Vascular endothelial growth factor (VEGF), which is produced by tumor cells, is a potent endothelial cell mitogen. The aim of the present study was to evaluate the response of orthotopic prostate cancer xenografts and prostate cancer bone metastasis to anti-VEGF receptor (flk-1) antibody (DC101) treatment.**

Experimental Design: **Orthotopic prostate cancer models (PC-3M-MM2 and LNCaP-LN3 prostate carcinoma cells) and a prostate cancer bone metastasis model (PC-3M-MM2) were used for these experiments. Early and established tumors were treated with saline, paclitaxel, DC101, or a DC101-plus-paclitaxel combination for 5 weeks (PC-3M-MM2) and 12 weeks (LNCaP-LN3). At the end of therapy, tumors were removed and weighed. Apoptosis, tumor cell proliferation, and angiogenesis- and metastasis-related gene expression were evaluated using immunohistochemistry, *in situ* hybridization, and terminal deoxynucleotidyl transferase-ediated nick end labeling (TUNEL).**

Results: **After treatment of early tumors (PC-3M-MM2), median prostate tumor weights (±SE) were 1230 ± 210 mg in untreated controls, 482 ± 121 mg in mice treated with paclitaxel ($P = 0.009$), 148 ± 27 mg in mice treated with DC101 ($P < 0.001$), and 48 ± 10 mg in mice treated with the combination of DC101 and paclitaxel ($P < 0.001$). Lymph node metastasis occurred in 7 of the 9 control mice, 5 of the 9 paclitaxel-treated animals, 5 of the 12 DC101-treated animals, and 2 of the 11 animals in the combination therapy group. Treatment with DC101 alone or in combination with paclitaxel reduced tumor-induced neovascularity measured by microvessel density and tumor cell proliferation (by proliferating cell nuclear antigen) and enhanced apoptosis (measured by TUNEL) in tumor cells and endothelial cells compared with controls. In the tibial prostate cancer metastasis model, significant inhibition of tumor growth was observed. In the LNCaP-LN3 orthotopic prostate cancer model, tumors occurred in 7 of the 10 control mice, 4 of the 10 paclitaxel-treated animals, 5 of the 10 DC101-treated animals, and 2 of the 11 animals in the combination therapy group ($P < 0.05$). The efficacy of DC101 was much greater in the treatment of early tumors, which suggests that tumor burden may be a critical factor in determining the response to DC101. *In vitro* and *in vivo* analysis of endothelial cell function showed reduced matrix metalloproteinase type 9 production in endothelial cells treated with DC101.**

Conclusions: **This study confirms the principle of tumor growth inhibition by targeting angiogenesis within tumors and supports the use of anti-VEGF receptor agents.**

INTRODUCTION

Prostate cancer remains a significant health problem with predictions for 198,100 new cases and 31,500 deaths in the United States in 2001 (1). Most advanced prostate cancers initially respond to androgen deprivation but ultimately follow a common pathway leading to androgen-independent disease. Limited therapeutic options exist at this stage of disease.

Tumor growth and metastasis depend on the ability of a tumor to recruit blood vessels for delivery of oxygen and nutrients (2). This process, angiogenesis, is driven by various growth factors (VEGF,[3] bFGF, insulin-like growth factor-1, angiopoi-

Received 3/1/02; revised 5/7/02; accepted 5/13/02.

The costs of publication of this article were defrayed in part by the payment of page charges. This article must therefore be hereby marked *advertisement* in accordance with 18 U.S.C. Section 1734 solely to indicate this fact.

[1] Supported by NIH Prostate Specialized Programs of Research Excellence (SPORE) CA90270-01; National Cancer Institute Core Grant CA 16672; a grant from ImClone Systems; the Department of Defense DAMD-17-98-1-8479; and by the Royal College of Surgeons in Ireland (Post Graduate Travel Grant) and the University of Dublin Post Graduate Traveling Scholarship (to P. S.)

[2] To whom requests for reprints should be addressed, at Department of Cancer Biology, Box 173, The University of Texas M. D. Anderson Cancer Center, 1515 Holcombe Boulevard, Houston, TX 77030. Phone: (713) 792-3250; Fax: (713) 792-8747; E-mail: cdinney@mdanderson.org.

[3] The abbreviations used are: VEGF, vascular endothelial cell growth factor; PCNA, proliferating cell nuclear antigen; TUNEL, TdT-mediated nick end labeling; MMP, matrix metalloproteinase; bFGF, basic fibroblast growth factor; IL, interleukin; VEGFR, VEGF receptor; IHC, immunohistochemical; MVD, microvessel density; ECM, extracellular matrix; ISH, *in situ* hybridization; TdT, terminal deoxynucleotidyltransferase; DAPI, 4′,6-diamidino-2-phenylindole.

etin-1, and epidermal growth factor), and cytokines (IL-8) and is facilitated by collagenase activity. Antiangiogenic molecules (including thrombospondin, IFNs, tissue inhibitors of MMPs, angiopoietin-2, endostatin, and angiostatin), impede angiogenesis. An angiogenic switch occurs when the tumor and stroma produce an excess of proangiogenic molecules over antiangiogenic factors (3). This "switch" favors the growth of new blood vessels and, thus, facilitates proliferation and growth of the tumor.

VEGF is produced by a variety of normal and neoplastic cells. It is a potent endothelial cell-specific mitogen and inhibits apoptosis of endothelial cells (4). It promotes invasion and migration of endothelial cells, and by increasing vascular permeability, it facilitates the entry of tumor cells into the circulation through which they can metastasize to distant sites. VEGF is produced in response to hypoxia and is regulated at a transcriptional level by hypoxia-inducible factor 1 (5). VEGF exists in several isoforms in the circulation and has 3 known receptors. The VEGFR-2, (flk-1, KDR) receptor was originally thought to be specific to endothelial cells and hemopoietic stem cells. However, recent studies have confirmed the presence of VEGFR-2/flk-1 on undifferentiated malignant melanoma and pancreatic tumor cells (6, 7). Ligand binding induces dimerization of the receptor and autophosphorylation of tyrosine kinase residues in the intracellular domain. VEGFR-2 signaling is poorly characterized but appears to act via the mitogen-activated protein kinase cascade to induce endothelial cell proliferation, via the phosphoinositide 3 kinase to activate an antiapoptotic pathway (8, 9), and via phospholipase Cγ (10).

The use of antibodies that neutralize VEGF, VEGFR blockers, dominant-negative receptor strategies, and tyrosine kinase inhibitors have helped elucidate the central role of VEGF in tumor angiogenesis (11–13). These proof-of-principle studies have lead the way for the evaluation of targeting the VEGF pathway as an antitumor strategy.

DC101 is a neutralizing monoclonal antibody that binds to the murine VEGFR-2/flk-1 receptor with high affinity and blocks ligand-induced receptor activation. Preclinical studies using DC101 have demonstrated considerable efficacy in inhibiting the growth of several human cancer xenografts (14–16). Our postulate was that DC101 would inhibit tumorigenesis by reducing angiogenesis in orthotopic prostate cancer xenografts. DC101 was used in combination with paclitaxel, which has demonstrated biochemical and objective responses in clinical trials with prostate cancer and which is a key component of many multiagent chemotherapy regimens for prostate cancer (17). In this study, we demonstrated reduced tumorigenicity and metastasis in orthotopic prostate cancer xenografts in nude mice treated with DC101. The inhibition of tumor growth was also confirmed in a bone metastasis model. This inhibition was potentiated by paclitaxel and was shown to result from reduced tumor cell proliferation, inhibition of angiogenesis, increased endothelial and tumor cell apoptosis, and decreased production of collagenases by endothelial cells.

MATERIALS AND METHODS

Cell Lines and Cultures. The highly metastatic, androgen-independent human prostate carcinoma cell line PC-3M-MM2 was grown as a monolayer in Eagle's MEM, supplemented with 10% fetal bovine serum, vitamins, sodium pyruvate, L-glutamine, nonessential amino acids, and penicillin-streptomycin. The relatively androgen-sensitive LNCaP-LN3 prostate carcinoma cells were grown in RPMI with similar supplements, and murine lung endothelial cells, immortalized by SV40 transformation, were grown in MEM with supplements (18).

Reagents. The monoclonal rat antimouse VEGFR-2 antibody DC101 was generously donated by ImClone Systems Incorporated (New York, NY; Refs. 19 and 20). Paclitaxel was purchased from Bristol-Myers Squibb Co. (Princeton, NJ).

***In Vitro* Analysis of mRNA MMP-9 Production by Endothelial Cells.** Murine lung endothelial cells were plated on autoclaved Probe-On slides (Fisher Scientific, Pittsburgh, PA) in a culture dish and grown to 60–70% confluency. The cells were incubated under serum-free conditions for 24 h and then in serum-free medium containing DC101 (25 and 50 nM) for 72 h. Human recombinant VEGF (R&D Systems, Minneapolis, MN; 20 ng/ml), was added to the medium for 2 h. After the slides were washed twice in PBS, they were fixed in 4% paraformaldehyde for 30 min at room temperature. The slides were then stored in 70% ethanol before ISH for MMP-9 mRNA.

Animals. Male athymic nude mice were obtained from the Animal Production Area of the National Cancer Institute, Frederick Cancer Research Facility (Frederick, MD). The mice were maintained in a laminar air-flow cabinet under specific pathogen-free conditions and used at 8 weeks of age. All of the facilities were approved by the American Association for Accreditation of Laboratory Animal Care in accordance with the current regulations and standards of the United States Department of Agriculture, the Department of Health and Human Services, and the NIH.

Orthotopic Implantation of Tumor Cells. Cultured PC-3M-MM2 and LNCaP-LN3 cells (60–70% confluent) were prepared for injection as described previously (21). Mice were anesthetized with i.p. sodium pentobarbital (90 mg/kg). Via a lower midline incision, 5×10^4 viable PC-3M-MM2 cells or 2×10^6 LNCaP-LN3 cells in 50 μl of HBSS were injected into the prostate (day 0). Formation of a bulla indicated a satisfactory injection. The incision was closed with a single layer of surgical clips.

***In Vivo* Therapy of Human Prostate Cancer Growing in the Prostate of Athymic Nude Mice: PC-3M-MM2 Model.** To investigate the effect of tumor burden on therapy, early (day 4, experiment 1) and established (day 14, experiment 2) prostate tumors were treated as per the schedule in Fig. 1. In each experiment at the beginning of therapy, five animals were killed, and their prostate glands were removed and assessed for the presence and size of tumors. The remaining animals were randomly assigned to one of four groups (10 mice per group): saline-treated controls; paclitaxel therapy only; DC101 therapy only; and combined therapy with DC101 and paclitaxel. Treatment continued for 4 weeks. At this point, the control animals had palpable tumors, and all of the animals were killed and necropsied. The prostate glands were removed and weighed and either fixed in 10% buffered formalin or placed in OCT compound (Miles Laboratories, Elkhart, IN) and frozen at −80°C. The intra-abdominal lymph nodes were removed, fixed in 10%

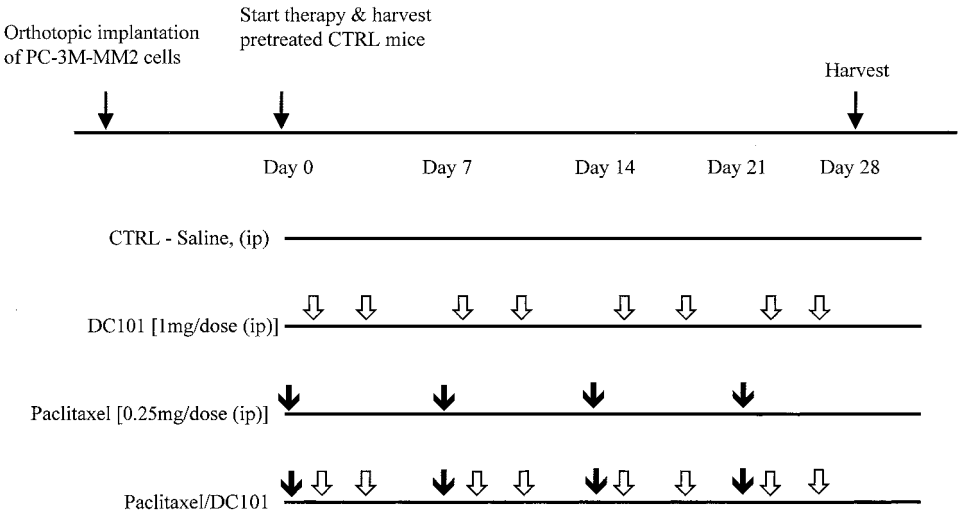

Fig. 1 Treatment schedule. Therapy began 4 days (Experiment 1) and 14 days (Experiment 2) after orthotopic prostate injection with PC-3M-MM2 cells (*Day 0*). In the tibial metastasis model, treatment began 4 days after tumor inoculation. Tumors were harvested from five animals at the time that therapy began. The remaining mice were randomly assigned to one of four treatment groups and were treated for 4 weeks according to the schedule. The remaining control and experimental mice were killed and necropsied 4 weeks later. (⇩, paclitaxel; ⇩, DC101)

buffered formalin, stained with H&E, and examined for the presence of metastasis.

***In Vivo* Therapy of Human Prostate Cancer Growing in the Prostate of Athymic Nude Mice: LNCaP-LN3 Model.** To investigate the response of a relatively androgen-sensitive cell line, mice bearing orthotopic LNCaP-LN3 prostate cancer xenografts were randomized to each of the four treatment groups described above. Because the LNCaP-LN3 tumors grow slowly, treatment began 1 month after tumor inoculation and continued for 12 weeks. Prostate glands were harvested as described above.

Tibial Prostate Carcinoma Metastasis Model. We used a semiquantitative model of metastatic prostate cancer that simulates a prostate cancer metastasis growing in a bone microenvironment. PC-3M-MM2 cells were prepared as described above. Mice were anesthetized using i.p. sodium pentobarbital. With the mouse grasped by the ankle, and the knee held in flexion, a 27-gauge needle was passed onto the articular surface of the tibia. With gentle pressure directed toward the tibial plateau, the needle was rotated. As the bony resistance was overcome, the tip of the needle passed into the intramedullary cavity of the tibia, and the inoculum of tumor cells was delivered (200,000 cells in 20 μl of HBSS). Removal of the needle was delayed for ~20 s after inoculation to allow the pressure in the intramedullary cavity to dissipate and to prevent extravasation of the tumor cells. Forty tibial injections were performed in 40 mice. These were randomized to the same treatment schedule as for the orthotopic prostate tumors (10 mice per group), with therapy commencing on day 4 (Fig. 1). No reliable method exists to quantify this type of tumor. The tibias were X-rayed at 2-week intervals for 6 weeks using a digital X-ray imaging system (MX-20; Faxitron X-ray Corporation, Wheeling, IL), after which the mice were killed. The tumors were removed and processed.

Colorimetric *in Situ* mRNA Hybridization. Specific antisense oligonucleotide DNA probes were designed complementary to the mRNA transcripts based on published reports of the cDNA sequence for VEGF/vascular permeability factor, bFGF, IL-8, E-cadherin, and MMP-9 (14). The specificity of the oligonucleotide sequence was initially determined by a GenBank European Molecular Library database and was also confirmed by Northern blot analysis (22). A poly $d(T)_{20}$ oligonucleotide was used to verify the integrity and lack of degradation of mRNA in each sample. All of the DNA probes were synthesized with six biotin molecules and were reconstituted to 1 μg/μl in a stock solution containing 10 mM Tris (pH 7.6) and 1 mM EDTA. *In situ* mRNA hybridization was performed using the Microprobe Manual Staining System (Fisher Scientific; Ref. 23) with minor modifications as described previously (22, 24). Briefly, tissue sections from PC-3M-MM2 tumors (4 μm) were dewaxed and rehydrated with Autodewaxer and Autoalcohol (Research Genetics), respectively, and then enzymatically digested with pepsin. Hybridization of the probe was performed for a total of 80 min at 45°C. The specimens were incubated with alkaline phosphatase-labeled avidin for 30 min at 45°C, rinsed with alkaline phosphatase enhancer for 1 min, and incubated with a chromogen substrate for 15 min at 45°C. A red stain indicated a positive reaction. Control for endogenous alkaline phosphatase included treatment of the sample in the absence of the biotinylated probe and use of chromogen alone.

Quantification of Color Reaction. Stained sections were examined using a Zeiss photomicroscope (Carl Zeiss, Thornwood, NY) equipped with a three-chip, charge-coupled device color camera (model DXC-969 MD; Sony Corp., Tokyo, Japan). Images were analyzed using Optimas image analysis software (version 4.10; Media Cybernetics, Silver Spring, MD). Images covering the range of staining intensities were captured electronically, and a color bar montage was created and threshold values were set in red green and blue. All of the subsequent images were quantified based on these threshold values. The integrated absorbance of each group was determined by examining five different fields in each sample to derive an average value. The intensity of staining was determined by comparison with the integrated absorbance of poly $d(T)_{20}$. The expression of each factor was presented relative to the control, which was arbitrarily assigned a value of 100 (25). The specimens were not

counterstained, so the absorbance was attributable solely to the product of the ISH reaction.

IHC Staining. For IHC analysis, frozen tissue sections from PC-3M-MM2 tumors (8 μm) were fixed in cold acetone. Formalin-fixed, paraffin-embedded specimens from PC-3M-MM2 tumors (5 μm) were deparaffinized in xylene and rehydrated in graded ethanol. Antigen retrieval was performed using pepsin for 12 min. Endogenous peroxidase activity was quenched with 3% hydrogen peroxide. Specimens were blocked with 5% normal horse serum plus 1% normal goat serum in PBS. The samples were incubated for 18 h at 4°C with one of the following: a 1:800 rat monoclonal anti-CD31 antibody (PharMingen, San Diego, CA), a 1:500 dilution of rabbit polyclonal anti-VEGF (Santa Cruz Biotechnology, Santa Cruz, CA), a 1:500 dilution of rabbit polyclonal bFGF antibody (Sigma Chemical Co., St. Louis, MO), a 1:50 dilution of a rabbit polyclonal anti-IL-8 antibody (Biosource International, Camarillo, CA), a 1:100 dilution of mouse monoclonal anti-MMP-9 antibody (Oncogene Research Products, Cambridge MA), or a 1:100 dilution of mouse monoclonal anti-PCNA antibody (DAKO, Carpinteria, CA). The samples were then rinsed four times with PBS before incubation with the appropriate secondary antibody: peroxidase-conjugated antirat IgG (H+L; Jackson ImmunoResearch Laboratory, West Grove, PA), antirabbit IgG, $F(ab')_2$ fragment (Jackson ImmunoResearch Laboratory), antimouse IgG1 (PharMingen), or antimouse IgG (Jackson ImmunoResearch Laboratory). The specimens were again rinsed with PBS and incubated with diaminobenzidine (Research Genetics) and mounted using universal mount (Research Genetics).

Quantification of Immunostaining Intensity. The intensity of the immunostaining for VEGF, bFGF, IL-8, and MMP-9 was measured in each treatment group using Optimas image analysis software (Media Cybernetics). Measurements were made in five different areas in each sample and quantified to yield an average measurement. The results are presented relative to the value for the control group, which was set at 100 (25).

Quantification of MVD. MVD was determined by light microscopy after immunostaining tissue sections from PC-3M-MM2 tumors with anti-CD31 antibodies according to the procedure of Weidner *et al.* (26). Clusters of stained endothelial cells distinct from adjacent microvessels, tumor cells, or other stromal cells were counted as one microvessel. The tissue was visualized using a cooled CCD Optronics Tec 470 camera (Optronic Engineering, Goletha, CA) linked to a computer and digital printer (Sony Corporation). The MVD was expressed as the average value for the five most densely staining areas identified within a single ×200 field.

TUNEL. Formalin-fixed, paraffin-embedded sections from PC-3M-MM2 tumors (5 μm) were deparaffinized in xylene and rehydrated in graded alcohol. The slides were rinsed with distilled water/BRIJ and treated with a 1:500 dilution of proteinase K (20 μg/ml) for 15 min; endogenous peroxidase was quenched with 3% hydrogen peroxide for 12 min. The samples were washed three times with distilled water/BRIJ and incubated for 10 min at room temperature with TdT buffer. Excess TdT buffer was drained, and the samples were incubated for 1 h at 37°C with terminal transferase (1:400) and biotin-16-dUTP (1:200) in TdT buffer. The samples were then rinsed twice with Tris buffer and incubated for 40 min at 37°C with a 1:400 dilution of peroxidase-conjugated streptavidin. The slides were incubated for 5 min with diaminobenzidine (Research Genetics).

Quantification of Cell Proliferation and Apoptosis. Cell proliferation and apoptosis were determined by immunohistochemistry with anti-PCNA antibodies and TUNEL. Tissue images were recorded using a cooled CCD Optronics Tec 470 camera linked to a computer and digital printer. The numbers of proliferative cells and apoptotic cells were expressed as the average value for the five most densely staining areas identified within a single ×200 field. An apoptosis to proliferation index was calculated.

Immunofluorescent Double-Staining of Apoptotic Endothelial Cells and Localization of Endothelial Cell MMP-9 Production. Frozen tissue sections from PC-3M-MM2 tumors (8 μm) were fixed with cold acetone for 5 min, acetone-chloroform (1:1, v/v) for 5 min, and acetone for 5 min. Samples were washed with PBS and incubated with protein-blocking solution containing 5% normal horse serum and 1% normal goat serum in PBS for 20 min. The tissues were incubated with a 1:800 dilution of rat monoclonal anti-CD31 antibody (PharMingen) for 24 h at 4°C. The samples were then rinsed with PBS and incubated with protein-blocking solution for 10 min before incubation for 1 h at room temperature with a 1:200 dilution of secondary goat antirat antibody conjugated to Texas Red (Jackson ImmunoResearch Laboratory). The specimens were washed in 0.1% Brij/PBS and then with PBS.

TUNEL was performed using a commercial kit (Promega, Madison, WI) with the following modifications. The CD31-labeled sections were fixed with 4% paraformaldehyde for 10 min at room temperature. They were then washed with PBS and incubated with 0.2% Triton X-100 for 15 min. After sections were washed twice with PBS, equilibration buffer was applied for 10 min. Reaction buffer containing equilibration buffer, nucleotide mixture, and TdT enzyme was added to the tissues, and the tissues were incubated in a humid atmosphere at 37°C for 1 h, avoiding exposure to light. The reaction was terminated by immersing the samples in 2× SSC for 15 min. The samples were then washed three times to remove unincorporated fluorescein-dUTP. To identify all of the cell nuclei, Vectashield mounting medium, DAPI (Vector Laboratories Inc., Burlingame, CA) was added to the slides and coverslips applied. The sections were examined under an Olympus Inverted System IX70 fluorescent microscope (Olympus, Melville, NY). Images were captured using a digital camera and Optimas software. Endothelial cells were identified by red fluorescence (600 nm); apoptosis was detected by the incorporation of fluorsecein-12-dUTP at the 3′-OH ends of fragmented DNA, resulting in localized green fluorescence (520 nm). Colocalization of the red and green fluorescence identified apoptotic endothelial cells, which appeared yellow.

To measure murine MMP-9 production by endothelial cells, tissue sections from PC-3M-MM2 tumors were labeled with anti-CD31/Texas Red as described above. The samples were then washed in PBS and blocked with 5% normal horse serum plus 1% normal goat serum. Samples were incubated overnight at 4°C with a 1:2000 rabbit antimouse MMP-9 antibody specific to the catalytic domain of murine MMP-9 (kindly

Table 1 Tumorigenicity and metastasis of orthotopic prostate xenografts[a]

	Experiment 1			Experiment 2		
Treatment group	Tumor incidence	Median tumor weight, mg (range)	Lymph node metastasis	Tumor incidence	Median tumor weight, mg (range)	Lymph node metastasis
Control	9/9	1230 (178–2225)	7/9	10/10	1142 (298–1960)	6/9
Paclitaxel	10/12	482 (152–1312)[b]	5/9	10/10	413 (109–1888)	7/11
DC101	8/12	148 (64–297)[b,c]	5/12	10/10	314 (53–741)[b]	5/6
Paclitaxel/DC101	7/11	48 (20–116)[b,c]	2/11[d]	10/10	399 (102–677)[b]	3/8

[a] The median tumor weight and range are reported only in those animals bearing tumors and are total prostate weight.
[b] $P < 0.01$ compared with control (Mann-Whitney U test).
[c] $P < 0.01$ compared with paclitaxel (Mann-Whitney U test).
[d] $P < 0.01$ compared with controls (χ^2 test).

donated by Dr. Robert Senior, Washington University, St. Louis, MO). The samples were then washed with PBS. After further protein blocking, the specimens were incubated with an antirabbit FITC-conjugated secondary antibody. DAPI (Vector Laboratories Inc.) was added to identify the nuclei, and the specimens were visualized with fluorescent microscopy as above (endothelial cells demonstrated localized red fluorescence and murine MMP-9 appeared green).

Statistical Analysis. The statistical differences for tumor size, MVD, proliferation, and apoptotic rates were analyzed by the Mann-Whitney U test. Staining intensity for bFGF, VEGF, IL-8, E-cadherin, and MMP-9, mRNA, and protein was also analyzed by the Mann-Whitney U test. Differences in the incidences of tumor and metastases between groups were analyzed by the χ^2 test. $P < 0.05$ was considered significant.

RESULTS

Orthotopic Prostate Cancer Model. DC101 therapy reduced the incidence, size, and metastatic potential of PC-3M-MM2 human prostate cancer xenografts growing in nude mice. In Experiment 1, the prostate glands removed from five animals before the initiation of treatment on day 4 had microscopic tumors. After completion of 4 weeks of therapy, the median tumor weight was 1230 mg in control animals but only 482 mg in paclitaxel-treated animals ($P = 0.009$, Mann Whitney U test). In the DC101-treated group, 8 of 12 animals developed tumors with a median weight of 148 mg ($P < 0.001$ compared with controls, Mann Whitney U test). In the DC101/paclitaxel combination therapy group, 7 of 11 animals developed tumors with a median weight of 48 mg ($P < 0.001$ compared with controls, Mann Whitney U test; Table 1). Lymph node metastases, confirmed by H&E staining, were found in 7 (77%) of 9 control mice, 5 (55%) of 9 paclitaxel-treated mice, 5 (42%) of 12 DC101-treated mice, and 2 (18%) of 11 mice that received combination therapy ($P < 0.01$, χ^2 test). In Experiment 2, treatment of established tumors began 14 days after tumor inoculation. Prostates harvested from five control animals at the beginning of therapy had macroscopic tumors with a median weight of 93 mg (range, 52–110 mg). Again, tumor weight was significantly lower in the mice treated with DC101 alone or in combination with paclitaxel. The statistically significant reduction in the incidence of lymph node metastasis observed when animals were treated at an early time point (day 4), Experiment 1, was not found in the treatment of established (day 14) tumors, Experiment 2.

In the orthotopic LNCaP-LN3 model, tumors developed in 7 of 10 in control mice, 4 of 10 paclitaxel-treated mice, 5 of 10 DC101-treated mice, and 2 of 11 mice that received combination therapy ($P < 0.05$, χ^2 test.)

Prostate Cancer Tibial Metastasis Model. There is no reliable method to objectively quantify tumor growing as a bone metastasis using the model described above. Therefore, we evaluated the response to treatment with serial X-rays performed 2, 4, and 6 weeks after tumor inoculation. Fig. 2 shows representative tibial X-rays in each group after 6 weeks of therapy. In the control group, there was extensive destruction of the proximal tibia and complete disruption of the knee joint. In the paclitaxel-treated group, substantial bony erosion was noted, similar to that found in the control animals. In the mice treated with DC101, either alone or in combination with paclitaxel, the amount of bone destruction was greatly reduced and the cortex was almost intact.

MVD/Endothelial Cell Apoptosis. CD31 immunostaining was used as a surrogate measure of angiogenesis. Significantly reduced MVD was demonstrated after therapy with paclitaxel, but the effect was much more remarkable with DC101, particularly when used in combination with paclitaxel (Table 2; Fig. 3). Using the double-fluorescent labeling strategy described above, we identified apoptotic endothelial cells only in the tumors of mice treated with DC101. Apoptotic endothelial cells were not identified in tumors from control or paclitaxel-treated mice (Fig. 3).

Tumor Cell Proliferation and Apoptosis. DC101 therapy, particularly when used in combination with paclitaxel, resulted in a significantly lower rate of tumor cell proliferation as measured by PCNA immunostaining. A similar effect of lesser magnitude was observed in the tumors treated with paclitaxel alone. TUNEL demonstrated significant increases in tumor cell apoptosis in the DC101-treated groups. The ratio of TUNEL:PCNA, which represents the balance between cell death and proliferation, was greatest in the combination treatment group (Table 2; Fig. 3).

The Effect of Therapy on Angiogenic Factor Expression. We evaluated the *in vivo* expression of mRNA and protein for the angiogenic and metastatic markers (IL-8, MMP-9, bFGF, VEGF, and E-cadherin) in orthotopic prostate cancer xenografts (Table 3). There was no significant alteration in the mRNA or protein expression for any of the factors after treatment with DC101, paclitaxel, or combination therapy compared with controls. This finding is in keep-

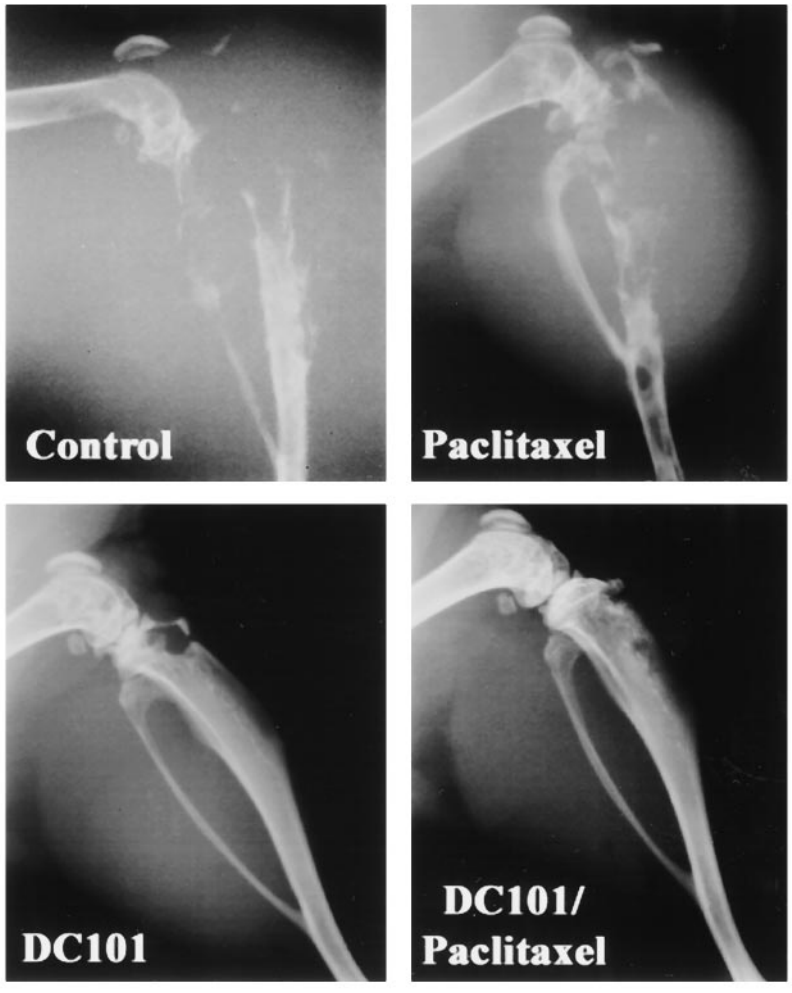

Fig. 2 Serial tibial X-rays were performed at 2-week intervals in mice bearing PC-3M-MM2 tumors. The films shown are representative of the treatment groups 6 weeks after tumor inoculation. In the control group and, to a lesser extent, in the paclitaxel-treated group, there were substantial bony erosions and disruption of the knee joint. In contrast, the extent of bony destruction in the DC101-treated tumors, both alone and in combination with paclitaxel, was markedly less.

Table 2 MVD, apoptosis, and cellular proliferation

Treatment group	MVD (median ± SE)	PCNA (median ± SE)	TUNEL (median ± SE)	TUNEL:PCNA ratio
Control	85 ± 1.8	168 ± 3.9	9 ± 1.1	5.4
Paclitaxel	55 ± 1.1[a]	130 ± 9.6[a]	13 ± 0.8[a]	10.1[b]
DC101	40 ± 1.0[b]	72 ± 4.3[b,c]	18 ± 3.0[b]	25.6[b,c]
Paclitaxel/DC101	32 ± 0.7[b,c]	54 ± 3.3[b,c]	16 ± 1.0[b,c]	29.6[b,c]

[a] $P < 0.05$ compared with controls (Mann-Whitney *U* test).
[b] $P < 0.01$ compared with control (Mann-Whitney *U* test).
[c] $P < 0.01$ compared with paclitaxel (Mann-Whitney *U* test).

ing with the selectivity of DC101 for murine endothelial cells because these factors are primarily produced by the human prostate cancer cells.

The Effect of Therapy on MMP-9 Production in Murine Endothelial Cells. We evaluated the effects of VEGFR blockade on murine endothelial cell MMP-9 expression *in vitro* and *in vivo*. ISH was used to quantify the production of MMP-9 mRNA in murine endothelial cells *in vitro*. After exposure to DC101 at 25 or 50 nM, murine MMP-9 mRNA levels were significantly reduced by 47 and 54%, respectively (Fig. 4).

We used a double-labeling procedure to colocalize endothelial cells and murine MMP-9 protein production in prostate tumor specimens *in vivo*. In untreated control tumors, murine MMP-9 was identified in the ECM adjacent to endothelial cells. In DC101-treated tumors, there was a reduction in endothelial cell-associated murine MMP-9 production (Fig. 5).

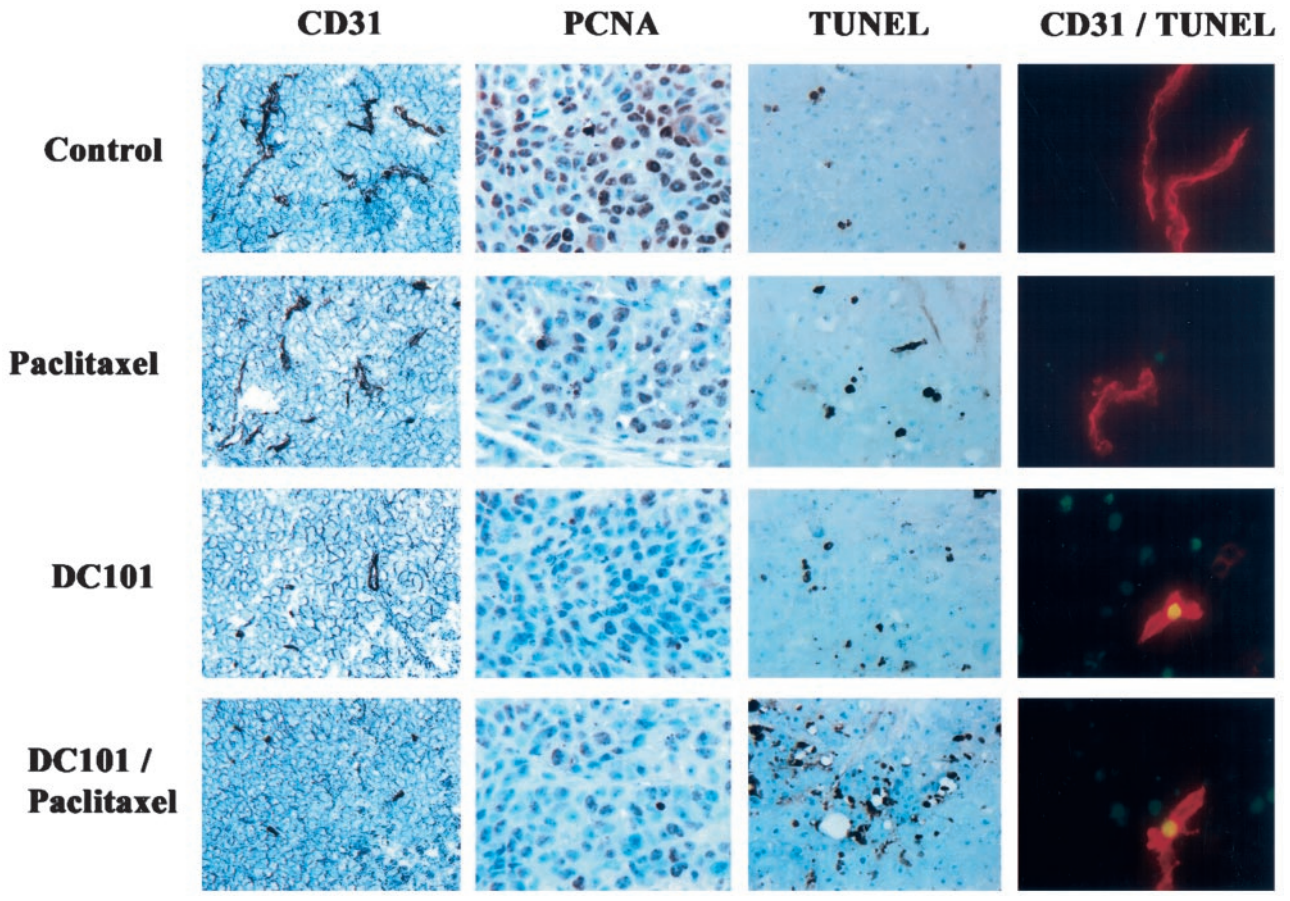

Fig. 3 Proliferation and apoptosis in PC-3M-MM2 xenografts were analyzed by IHC with anti-PCNA antibody and TUNEL. The average number of PCNA-positive cells per ×200 field decreased significantly from 168 in controls to 130, 72, and 54 in paclitaxel, DC101, and combination therapy groups, respectively. The number of apoptotic tumor cells increased significantly from 9 per ×200 field in controls to 13, 18, and 16 in the paclitaxel, DC101, and combination therapy groups, respectively. MVD in the treatment groups was measured by counting the average number of $CD31^+$ cells in five ×200 fields. MVD decreased significantly from 85 in controls to 55, 40, and 32 in the paclitaxel, DC101, and combination therapy groups, respectively. Endothelial cell apoptosis was detected by a double-labeling strategy in which endothelial cells were identified by using an anti-CD31 antibody (revealing *red fluorescence*), and apoptotic nuclei were detected by TUNEL assay (revealing *green fluorescence*). Colocalization of apoptotic endothelial cells was detected by a *yellow* coloration. Apoptotic endothelial cells were identified only in the tumors treated with DC101.

Table 3 mRNA and protein expression for MMP-9, VEGF, bFGF, IL-8, and E-cadherin after therapy with DC101 and paclitaxel

ISH was performed on two prostates from each group. Image analysis was carried out on five areas in each prostate. Expression of each factor in the tumor tissue was normalized by dividing by the expression of poly $d(T)_{20}$ in the same area. Immunohistochemistry was performed on two prostates from each group. Image analysis was carried out on five areas in each prostate. The expression of each factor is then presented relative to its expression in the control group, which is arbitrarily assumed to be 100%.

	mRNA expression					Protein expression			
Treatment group	MMP-9	VEGF	bFGF	IL-8	E-Cadherin	MMP-9	VEGF	bFGF	IL-8
Control	100	100	100	100	100	100	100	100	100
Paclitaxel	107	110	91	90	101	105	98	97	103
DC101	101	105	94	93	110	103	107	94	94
Paclitaxel/DC101	99	97	98	99	100	98	105	92	98

DISCUSSION

Surgical extirpation and radiation therapy are potentially curative treatment modalities for clinically localized prostate cancer. Currently, there is no curative therapy for locally advanced or metastatic prostate cancer. Combination chemotherapy produces minimal objective responses and rapidly leads to the development of drug resistance (27). Hormonal therapy has a limited role, and its effect is short lived as the selection of resistant clones occurs. Hence, the development of new therapeutic strategies including antiangiogenic therapy is urgently needed.

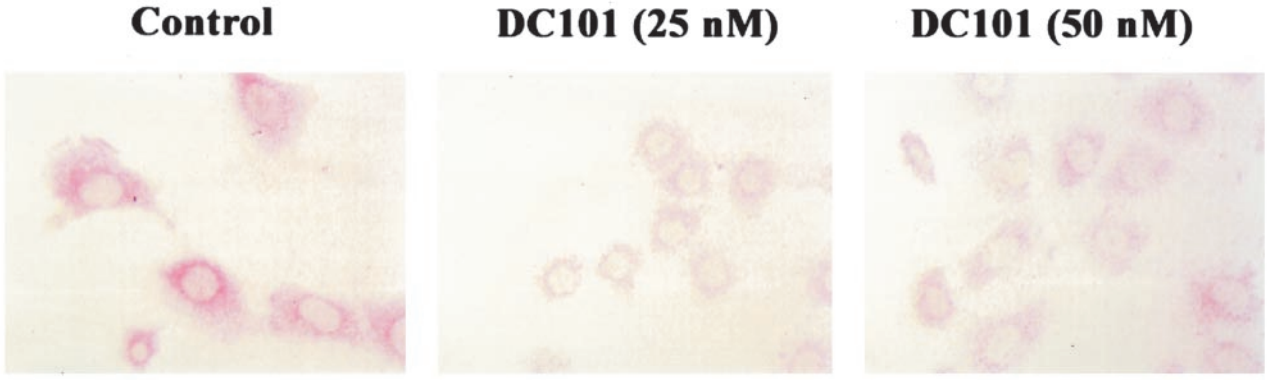

Fig. 4 Murine lung endothelial cells treated with DC101 (25 and 50 nM) were analyzed for MMP-9 mRNA expression using a colorimetric ISH procedure. Therapy with DC101 for 72 h significantly reduced MMP-9 mRNA expression in murine endothelial cells by 47% [*DC101 (25 nM)*] and 54% [*DC101 (50 nM)*].

The importance of VEGF in promoting the growth and metastasis of prostate cancer has been clearly elucidated. Several groups have shown increased expression of VEGF in prostate cancer cell lines growing in culture compared with benign prostate cells, with the highest expression noted in androgen-insensitive metastatic cell lines (28, 29). In our laboratory, using recycled prostate carcinoma cell variants in an orthotopic prostate cancer xenograft model, we have demonstrated an association between the invasive and metastatic potential of a cell line and VEGF expression (30). Clinical progression of prostate cancer and angiogenesis development has been linked in the transgenic adenocarcinoma of mouse prostate (TRAMP) model, in which development of a more malignant phenotype was associated with increasing production of VEGF and a change in the predominant VEGFR from VEGFR-1 to VEGFR-2/flk-1 (31). In clinical studies, urinary and serum VEGF levels have shown promise as prognostic markers, particularly in men with hormone-refractory prostate cancer (32, 33). The analysis of radical prostatectomy specimens by IHC analysis (34) and colorimetric ISH (35) has shown a significant association between VEGF expression and tumor grade and stage, as well as a positive correlation with clinical outcome.

The production of MMP-9 and other proteases by prostate cancer cells and stromal cells facilitates the degradation of the ECM, resulting in tumor invasion and subsequent metastasis (36, 37). MMPs are expressed by and around blood vessels, and changes in MMP activity modulate microtubule formation *in vitro* (38). The proteolytic effects of MMPs facilitate the migration of endothelial cells through the altered ECM toward angiogenic stimuli; in this manner, MMPs are an integral part of the angiogenesis process (39). Direct experimental evidence for the involvement of MMPs in angiogenesis came from analyses of mice made MMP-9-deficient by targeted mutagenesis (40). These mice demonstrated a delayed release of an angiogenic activator, thereby establishing that MMP-9 regulates angiogenesis. Using biochemically manipulated cells that produce less MMP-9, Sehgal *et al.* (36) have demonstrated in a murine prostate cancer model that MMP-9 expression is essential for the development of hematogenous metastasis. Although benign and hyperplastic prostatic tissues express negligible amounts of MMPs (41), malignant and metastatic prostatic tissues express relatively greater amount of MMPs (42). The magnitude of collagenase production by prostate carcinoma cells has been linked to their invasive and metastatic potential (43). Some authors have reported a correlation between MMP-9 expression and stage (35) and a possible independent predictive prognostic value for MMP expression in prostate carcinomas (44). Thus the production of MMP-9 and VEGF are intrinsically linked to tumor angiogenesis, growth, and progression, and these molecules are, therefore, valid targets for novel therapeutic strategies in prostate cancer.

In the present study, using orthotopic models of prostate cancer and prostate cancer bone metastasis, we demonstrated significant growth inhibition and reduction in metastatic potential of early orthotopic xenografts growing in the prostate gland of athymic nude mice treated with DC101. We extended our study to include treatment of well-established macroscopic tumors and again demonstrated significant inhibition of growth. The incidence of lymph node metastasis in the established tumors was not reduced by DC101 therapy, which suggests that metastasis in this model may be an early event or that lymphatic dissemination occurs independently of therapy as a function of tumor burden. Furthermore, the growth-inhibitory effects of DC101 have been confirmed in two cell lines that have different degrees of androgen sensitivity. The growth of bony prostate metastases in the tibia of nude mice was also inhibited by treatment with DC101. These models most closely simulate the *in vivo* conditions of prostate cancer growing in its native microenvironment and allow critical tumor-stromal interactions to be recreated and studied. However, a limitation of these types of models is the lack of an intact immune system in nude mice that may have a role in modulating therapeutic and toxic effects.

In our study, we have shown that DC101 acts by reducing MVD via the induction of endothelial cell apoptosis and by decreasing the production of MMP-9 by endothelial cells. Reduced proliferation and increased apoptosis in these tumors are presumably secondary to the antiangiogenic effects. The therapeutic effects were much more marked in Experiment 1 of our study. Established tumors appeared less sensitive to the effects of VEGF blockade. The difference in response may relate to the

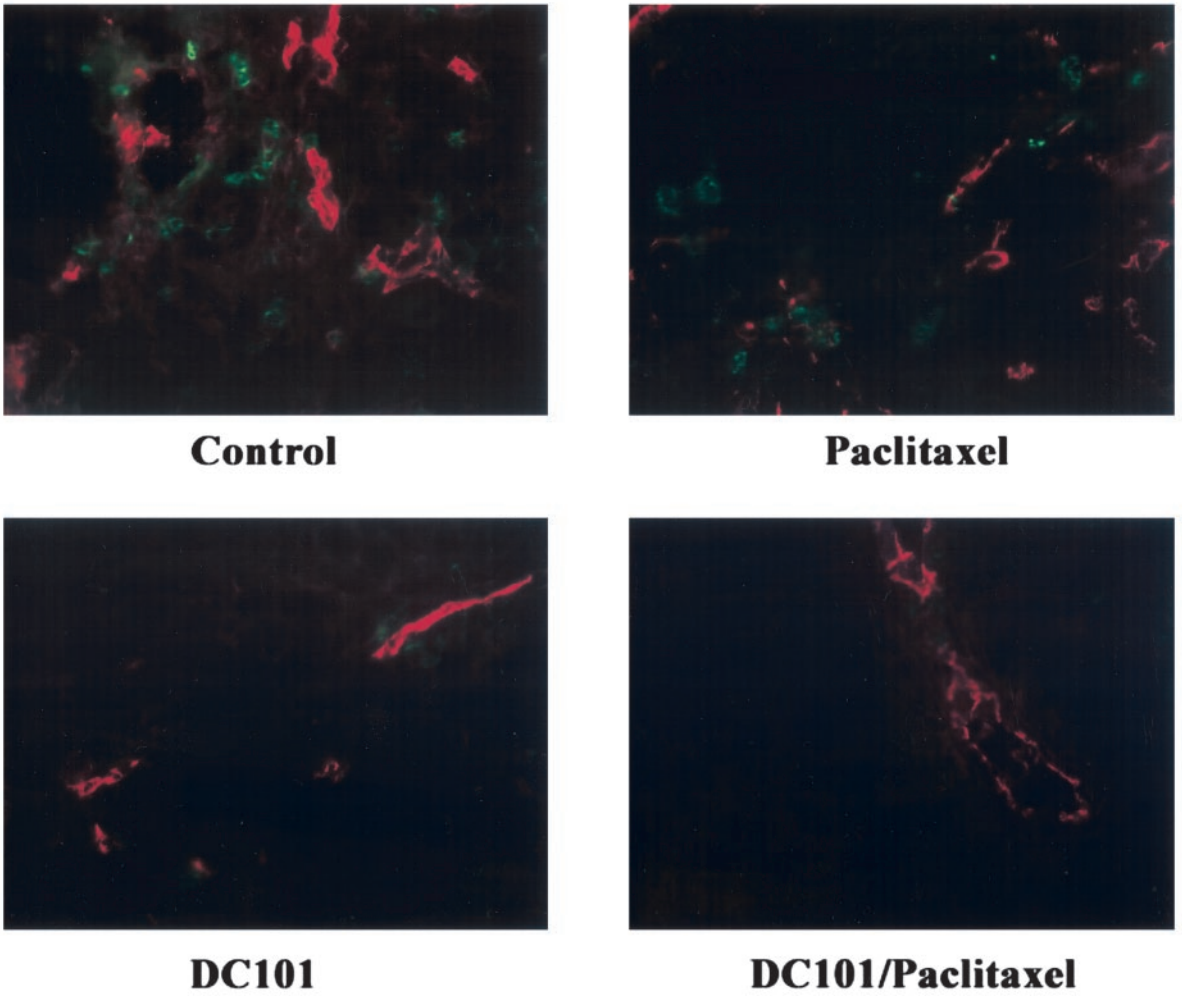

Fig. 5 *In vivo* PC-3M-MM2 tumor specimens were stained using anti-CD31 antibodies and a Texas red fluorescent secondary antibody to label endothelial cells (*red*). A murine-specific MMP-9 antibody linked to a *green fluorescent* secondary antibody was used to identify MMP-9 of murine origin (from stromal cells). MMP-9, a secreted zymogen, was detected in and around the endothelial cells. In the tumors treated with DC101, there was markedly reduced MMP-9 production.

greater reliance of immature endothelial cells on the trophic support of VEGF, as reported by Tran *et al.* (45). These findings have implications for the introduction of antiangiogenic agents in clinical trials. Because these agents have much greater efficacy against immature endothelium, it may be prudent to explore their role not only as an adjuvant therapy for advanced tumors but also in a chemoprevention setting in which angiogenesis is critical for tumor initiation.

The present study demonstrated the regulation of MMP-9 production in endothelial cells by DC101. Dias *et al.* (46) have previously shown that MMP-9 production in leukemic cells is dependent on VEGF stimulation and that, by decreasing collagenase production via VEGF deprivation, leukemic cell migration, although an artificial ECM, is impaired. Leukemic and endothelial cells share a common precursor cell and express the same VEGFRs, and, thus, similar signal transduction pathways may be involved in this effect. Our findings from IHC analysis and ISH clearly show regulation of MMP-9 production in endothelial cells by DC101 (Figs. 4 and 5). However, alternative sources of MMP-9 (including other stromal elements and tumor cells) were not affected by DC101, and the immunostaining of whole tumors did not show any significant change in MMP-9 production (Table 3).

DC101, a chimeric form of the VEGFR-2 receptor antibody, has entered Phase I clinical studies in colorectal cancer. The development of novel biological therapies in the last few years has led to new paradigms for the design and evaluation of clinical studies. Many of these biological agents are cytostatic and do not cause regression of established tumors but, rather, delay tumor growth. As a result, biological agents entering clinical trials are now being evaluated as chronic or maintenance therapy. In addition, these agents are being combined with conventional chemotherapeutic agents or radiation therapy. The present study, in addition to others (14), has demonstrated synergistic responses by targeting both components of the tumor: the cancer cells and the supporting stroma.

Established criteria used to evaluate cytotoxic chemotherapeutic agents (toxicity and response rates) may be inappropriate for biological agents. The traditional end points have been replaced by measurement of time-to-disease-progression, usually combined with some surrogate marker of response, such as MVD in the case of antiangiogenic therapy (47). Biological therapies and, in particular, antiangiogenic therapy offer advantages over traditional chemotherapy. The majority of the agents can be given p.o., and minimal toxic effects have been reported in preclinical and clinical trials. Drug resistance has not been observed because of the lower turnover rate and reduced propensity for genetic instability in endothelial cells compared with tumor cells. Future developments in antiangiogenic therapy will lead to targeted therapy to avoid physiological angiogenic processes.

In conclusion, therapy with DC101, a monoclonal antibody to the flk-1 receptor, inhibited the growth and metastasis of orthotopic prostate cancer xenografts in athymic nude mice. The growth of simulated prostate cancer bone metastases in the tibia of nude mice was likewise inhibited by treatment with DC101. Treatment with DC101 reduced MVD via the induction of endothelial cell apoptosis and decreased the production of MMP-9 by endothelial cells. The tumors in mice treated with DC101 showed diminished angiogenesis, lower cellular proliferation rates, and significantly greater tumor and endothelial cell apoptosis. These results validate the concept of targeting the vascular endothelium as a means of inhibiting the growth and metastasis of prostate cancer.

REFERENCES

1. Greenlee, R. T., Hill-Harmon, M. B., Murray, T., and Thun, M. Cancer Statistics 2001. CA Cancer J., *51:* 15–36, 2001.

2. Folkman, J. Tumor angiogenesis: therapeutic implications. N. Engl. J. Med., *285:* 1182–1186, 1971.

3. Hanahan, D., and Folkman, J. Patterns and emerging mechanisms of the angiogenic switch during tumorigenesis. Cell, *86:* 353–364, 1996.

4. Neufeld, G., Cohen, T., Gengrinovitch, S., and Poltorak, Z. Vascular endothelial growth factor (VEGF) and its receptors. FASEB J., *13:* 9–22, 1999.

5. Levy, A. P., Levy, N. S., Wegner, S., and Goldberg, M. A. Transcriptional regulation of the rat *vascular endothelial growth factor* gene by hypoxia. J. Biol. Chem., *270:* 13333–13340, 1995.

6. von Marschall, Z., Cramer, T., Hocker, M., Burde, R., Plath, T., Schirner, M., Heidenreich, R., Breier, G., Riecken, E. O., Wiedenmann, B., and Rosewicz, S. *De novo* expression of vascular endothelial growth factor in human pancreatic cancer: evidence for an autocrine mitogenic loop. Gastroenterology, *119:* 1358–1372, 2000.

7. Lacal, P. M., Failla, C. M., Pagani, E., Odorisio, T., Schietroma, C., Falcinelli, S., Zambruno, G., and D'Atri, S. Human melanoma cells secrete and respond to placenta growth factor and vascular endothelial growth factor. J. Investig Dermatol., *115:* 1000–1007, 2000.

8. Kroll, J., and Waltenberger, J. The vascular endothelial growth factor receptor KDR activates multiple signal transduction pathways in porcine aortic endothelial cells. J. Biol. Chem., *272:* 32521–32527, 1997.

9. Gerber, H. P., McMurtrey, A., Kowalski, J., Yan, M., Keyt, B. A., Dixit, V., and Ferrara, N. Vascular endothelial growth factor regulates endothelial cell survival through the phosphatidylinositol 3′-kinase/Akt signal transduction pathway. Requirement for Flk-1/KDR activation. J. Biol. Chem., *273:* 30336–30343, 1998.

10. Takahashi, T., Ueno, H., and Shibuya, M. VEGF activates protein kinase C-dependent, but Ras-independent Raf-MEK-MAP kinase pathway for DNA synthesis in primary endothelial cells. Oncogene, *18:* 2221–2230, 1999.

11. Kim, K. J., Li, B., Winer, J., Armanini, M., Gillett, N., Phillips, H. S., and Ferrara, N. Inhibition of vascular endothelial growth factor-induced angiogenesis suppresses tumour growth *in vivo*. Nature (Lond.), *362:* 841–844, 1993.

12. Millauer, B., Shawver, L. K., Plate, K. H., Risau, W., and Ullrich, A. Glioblastoma growth inhibited *in vivo* by a dominant-negative Flk-1 mutant. Nature (Lond.), *367:* 576–579, 1994.

13. Melnyk, O., Zimmerman, M., Kim, K. J., and Shuman, M. Neutralizing anti-vascular endothelial growth factor antibody inhibits further growth of established prostate cancer and metastases in a pre-clinical model. J. Urol., *161:* 960–963, 1999.

14. Inoue, K., Slaton, J. W., Davis, D. W., Hicklin, D. J., McConkey, D. J., Karashima, T., Radinsky, R., and Dinney, C. P. Treatment of human metastatic transitional cell carcinoma of the bladder in a murine model with the anti-vascular endothelial growth factor receptor monoclonal antibody DC101 and paclitaxel. Clin. Cancer. Res., *6:* 2635–2643, 2000.

15. Bruns, C. J., Liu, W., Davis, D. W., Shaheen, R. M., McConkey, D. J., Wilson, M. R., Bucana, C. D., Hicklin, D. J., and Ellis, L. M. Vascular endothelial growth factor is an *in vivo* survival factor for tumor endothelium in a murine model of colorectal carcinoma liver metastases. Cancer (Phila.), *89:* 488–499, 2000.

16. Shaheen, R. M., Tseng, W. W., Vellagas, R., Liu, W., Ahmad, S. A., Jung, Y. D., Reinmuth, N., Drazan, K. E., Bucana, C. D., Hicklin, D. J., and Ellis, L. M. Effects of an antibody to vascular endothelial growth factor receptor-2 on survival, tumor vascularity, and apoptosis in a murine model of colon carcinomatosis. Int. J. Oncol., *18:* 221–226, 2001.

17. Hudes, G. R., Nathan, F., Khater, C., Haas, N., Cornfield, M., Giantonio, B., Greenberg, R., Gomella, L., Litwin, S., Ross, E., Roethke, S., and McAleer, C. Phase II trial of 96-hour paclitaxel plus oral estramustine phosphate in metastatic hormone-refractory prostate cancer. J. Clin. Oncol., *15:* 3156–3163, 1997.

18. Pettaway, C. A., Pathak, S., Greene, G., Ramirez, E., Wilson, M. R., Killion, J. J., and Fidler, I. J. Selection of highly metastatic variants of different human prostatic carcinomas using orthotopic implantation in nude mice. Clin. Cancer Res., *2:* 1627–1636, 1996.

19. Witte, L., Hicklin, D. J., Zhu, Z., Pytowski, B., Kotanides, H., Rockwell, P., and Bohlen, P. Monoclonal antibodies targeting the VEGF receptor-2 (Flk1/KDR) as an anti-angiogenic therapeutic strategy. Cancer Metastasis Rev., *17:* 155–161, 1998.

20. Prewett, M., Huber, J., Li, Y., Santiago, A., O'Connor, W., King, K., Overholser, J., Hooper, A., Pytowski, B., Witte, L., Bohlen, P., and Hicklin, D. J. Antivascular endothelial growth factor receptor (fetal liver kinase 1) monoclonal antibody inhibits tumor angiogenesis and growth of several mouse and human tumors. Cancer Res., *59:* 5209–5218, 1999.

21. Delworth, M. G., Nishioka, K., Pettaway, C. A., Gutman, M., Killion, J. J., von Eschenbach, A. C., and Fidler, I. J. Systemic administration of 4-amidinoindanon-1-(2′-amidino)-hydrazone, a new inhibitor of *S*-adenosylmethionine decarboxylase, produces cytostasis of human prostate cancer in athymic nude mice. Int. J. Oncol., *6:* 293–299, 1995.

22. Radinsky, R., Bucana, C. D., Ellis, L. M., Sanchez, R., Cleary, K. R., Brigati, D. J., and Fidler, I. J. A rapid colorimetric *in situ* messenger RNA hybridization technique for analysis of epidermal growth factor receptor in paraffin-embedded surgical specimens of human colon carcinomas. Cancer Res., *53:* 937–943, 1993.

23. Reed, J. A., Manahan, L. J., Park, C. S., and Brigati, D. J. Complete one-hour immunocytochemistry based on capillary action. Biotechniques, *13:* 434–443, 1992.

24. Bucana, C. D., Radinsky, R., Dong, Z., Sanchez, R., Brigati, D. J., and Fidler, I. J. A rapid colorimetric *in situ* mRNA hybridization technique using hyperbiotinylated oligonucleotide probes for analysis of mdr1 in mouse colon carcinoma cells. J Histochem. Cytochem., *41:* 499–506, 1993.

25. Perrotte, P., Matsumoto, T., Inoue, K., Kuniyasu, H., Eve, B. Y., Hicklin, D. J., Radinsky, R., and Dinney, C. P. Anti-epidermal growth

factor receptor antibody C225 inhibits angiogenesis in human transitional cell carcinoma growing orthotopically in nude mice. Clin. Cancer Res., *5:* 257–265, 1999.

26. Weidner, N., Carroll, P. R., Flax, J., Blumenfeld, W., and Folkman, J. Tumor angiogenesis correlates with metastasis in invasive prostate carcinoma. Am. J. Pathol., *143:* 401–409, 1993.

27. Yagoda, A., and Petrylak, D. Cytotoxic chemotherapy for advanced hormone-resistant prostate cancer. Cancer (Phila.), *7:* 1098–1109, 1993.

28. Chen, H. J., Treweeke, A. T., Ke, Y. Q., West, D. C., and Toh, C. H. Angiogenically active vascular endothelial growth factor is overexpressed in malignant human and rat prostate carcinoma cells. Br. J. Cancer, *82:* 1694–1701, 2000.

29. Haggstrom, S., Bergh, A., and Damber, J. E. Vascular endothelial growth factor content in metastasizing and nonmetastasizing Dunning prostatic adenocarcinoma. Prostate, *45:* 42–50, 2000.

30. Balbay, M. D., Pettaway, C. A., Kuniyasu, H., Inoue, K., Ramirez, E., Li, E., Fidler, I. J., and Dinney, C. P. Highly metastatic human prostate cancer growing within the prostate of athymic mice overexpresses vascular endothelial growth factor. Clin. Cancer Res., *5:* 783–789, 1999.

31. Huss, W. J., Hanrahan, C. F., Barrios, R. J., Simons, J. W., and Greenberg, N. M. Angiogenesis and prostate cancer: identification of a molecular progression switch. Cancer Res., *61:* 2736–2743, 2001.

32. Bok, R. A., Halabi, S., Fei, D. T., Rodriquez, C. R., Hayes, D. F., Vogelzang, N. J., Kantoff, P., Shuman, M. A., and Small, E. J. Vascular endothelial growth factor and basic fibroblast growth factor urine levels as predictors of outcome in hormone-refractory prostate cancer patients: a cancer and leukemia group B study. Cancer Res., *61:* 2533–2536, 2001.

33. Jones, A., Fujiyama, C., Turner, K., Fuggle, S., Cranston, D., Bicknell, R., and Harris, A. L. Elevated serum vascular endothelial growth factor in patients with hormone-escaped prostate cancer. BJU Int., *85:* 276–280, 2000.

34. Strohmeyer, D., Rossing, C., Bauerfeind, A., Kaufmann, O., Schlechte, H., Bartsch, G., and Loening, S. Vascular endothelial growth factor and its correlation with angiogenesis and p53 expression in prostate cancer. Prostate, *45:* 216–224, 2000.

35. Kuniyasu, H., Troncoso, P., Johnston, D., Bucana, C. D., Tahara, E., Fidler, I. J., and Pettaway, C. A. Relative expression of type IV collagenase. E-cadherin, and vascular endothelial growth factor/vascular permeability factor in prostatectomy specimens distinguishes organ-confined from pathologically advanced prostate cancers. Clin. Cancer Res., *6:* 2295–2308, 2000.

36. Sehgal, G., Hua, J., Bernhard, E. J., Sehgal, I., Thompson, T. C., and Muschel, R. J. Requirement for matrix metalloproteinase-9 (gelatinase B) expression in metastasis by murine prostate carcinoma. Am. J. Pathol., *152:* 591–596, 1998.

37. Stearns, M. E., and Stearns, M. Immunohistochemical studies of activated matrix metalloproteinase-2 (MMP-2a)expression in human prostate cancer. Oncol. Res., *8:* 63–67, 1996.

38. Karelina, T. V., Goldberg, G. I., and Eisen, A. Z. Matrix metalloproteinases in blood vessel development in human fetal skin and in cutaneous tumors. J. Investig Dermatol., *105:* 411–417, 1995.

39. Fisher, C., Gilbertson-Beadling, S., Powers, E. A., Petzold, G., Poorman, R., and Mitchell, M. A. Interstitial collagenase is required for angiogenesis *in vitro*. Dev. Biol., *162:* 499–510, 1994.

40. Vu, T. H., Shipley, J. M., Bergers, G., Berger, J. E., Helms, J. A., Hanahan, D., Shapiro, S. D., Senior, R. M., and Werb, Z. MMP-9/gelatinase B is a key regulator of growth plate angiogenesis and apoptosis of hypertrophic chondrocytes. Cell, *93:* 411–422, 1998.

41. Stearns, M. E., and Wang, M. Type IV collagenase (M_r 72, 000) expression in human prostate: benign and malignant tissue. Cancer Res., *53:* 878–883, 1993.

42. Hamdy, F. C., Fadlon, E. J., Cottam, D., Lawry, J., Thurrell, W., Silcocks, P. B., Anderson, J. B., Williams, J. L., and Rees, R. C. Matrix metalloproteinase 9 expression in primary human prostatic adenocarcinoma and benign prostatic hyperplasia. Br. J. Cancer, *69:* 177–182, 1994.

43. Boag, A. H., and Young, I. D. Immunohistochemical analysis of type IV collagenase expression in prostatic hyperplasia and adenocarcinoma. Mod. Pathol., *6:* 65–68, 1993.

44. Wood, M., Fudge, K., Mohler, J. L., Frost, A. R., Garcia, F., Wang, M., and Stearns, M. E. *In situ* hybridization studies of metalloproteinases 2 and 9 and TIMP-1 and TIMP-2 expression in human prostate cancer. Clin. Exp. Metastasis, *15:* 246–258, 1997.

45. Tran, J., Rak, J., Sheehan, C., Saibil, S. D., LaCasse, E., Korneluk, R. G., and Kerbel, R. S. Marked induction of the IAP family antiapoptotic proteins survivin and XIAP by VEGF in vascular endothelial cells. Biochem. Biophys. Res. Commun., *264:* 781–788, 1999.

46. Dias, S., Hattori, K., Zhu, Z., Heissig, B., Choy, M., Lane, W., Wu, Y., Chadburn, A., Hyjek, E., Gill, M., Hicklin, D. J., Witte, L., Moore, M. A., and Rafii, S. Autocrine stimulation of VEGFR-2 activates human leukemic cell growth and migration. J. Clin. Investig., *106:* 511–521, 2000.

47. Herbst, R. S., Lee, A. T., Tran, H. T., and Abbruzzese, J. L. Clinical studies of angiogenesis inhibitors: the University of Texas MD Anderson Center Trial of Human Endostatin. Curr. Oncol. Rep., *3:* 131–140, 2001.